

**Supplementary Information**

**Stabilising Gallium-based Liquid Metal Alloy Nanoparticles by Carbon Encapsulation**

Imtisal Zahid<sup>a</sup>, Karma Zuraiqi<sup>a\*</sup>, Caiden J. Parker<sup>a</sup>, Muhammad Hamza Nazir<sup>a</sup>, Pierre H. A. Vaillant<sup>b</sup>, Edwin L. H. Mayes<sup>b</sup>, Ali Zavabeti<sup>a</sup>, Susanne Wintzheimer<sup>d,e</sup>, Vaishnavi Krishnamurthi<sup>a</sup>, Dan Yang<sup>c</sup>, Aaron Elbourne<sup>b</sup>, Ken Chiang<sup>a\*</sup>, Torben Daeneke<sup>a\*</sup>

<sup>a</sup>Department of Chemical and Environmental Engineering, School of Engineering RMIT University, Melbourne, VIC 3001, Australia

<sup>b</sup>School of Science RMIT University Melbourne, VIC 3001, Australia

<sup>c</sup>School of Engineering, Chemical Engineering, The University of Western Australia (M017), 6009 Perth, Australia

<sup>d</sup>Department of Chemistry and Pharmacy, Friedrich-Alexander-Universität Erlangen-Nürnberg (FAU), Egerlandstraße 1, 91058 Erlangen, Germany

<sup>e</sup>Fraunhofer-Institute for Silicate Research ISC, Neunerplatz 2, 97082 Würzburg, Germany

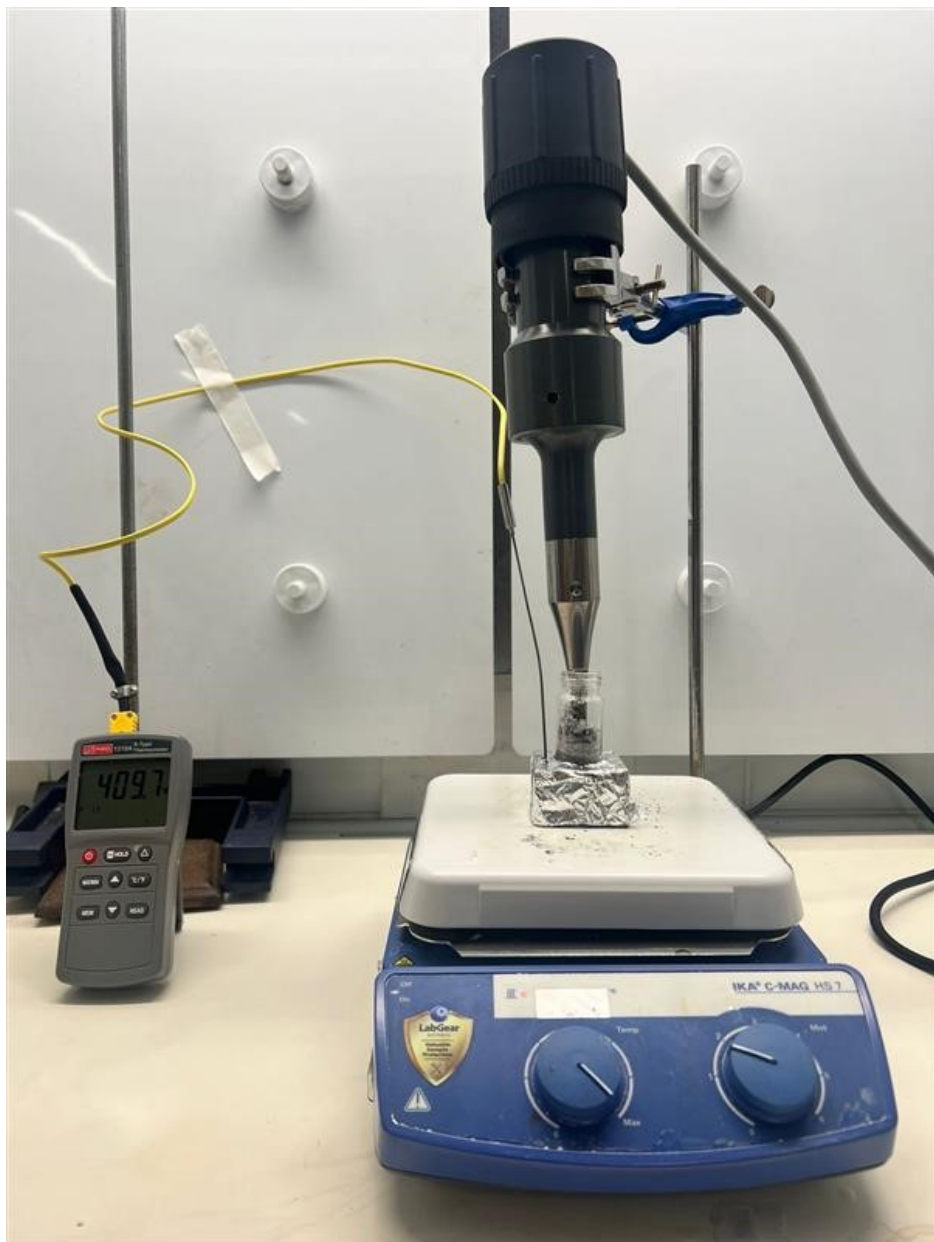


**Figure S1.** Synthesis setup for bimetallic and trimetallic LM NPs.

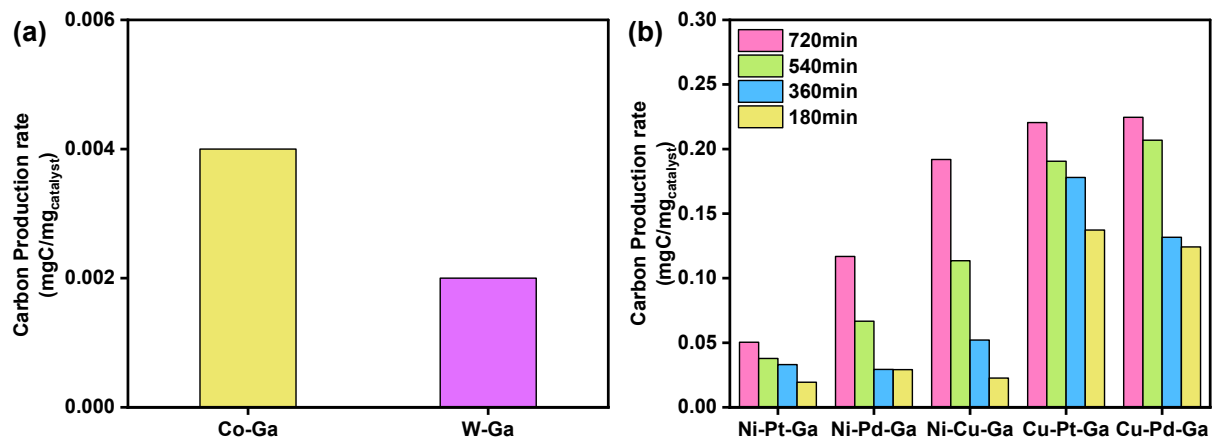


**Figure S2.** Methane pyrolysis at the following reaction conditions: 600 °C, 0.1L min<sup>-1</sup> gas flow of 4% methane/argon over various binary and ternary catalysts (a) Carbon production rate over Co-Ga and W-Ga, (b) Carbon production at different time intervals in the presence of ternary alloy nanoparticles (NPs).

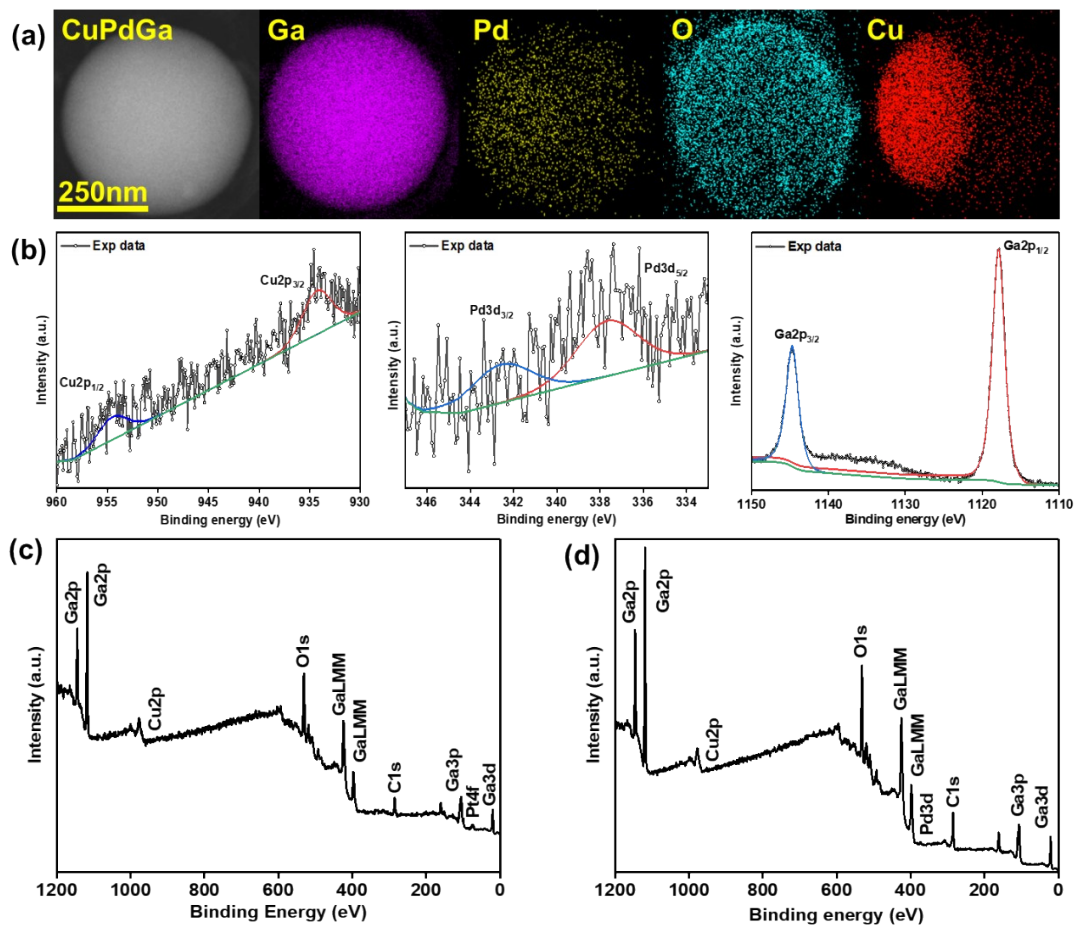


**Figure S3.** Surface and elemental analysis of the pristine Cu-Pd-Ga (3.0:0.5:96.5)

nanoparticle (NP), (a) Dark-field Transmission electron microscopy (TEM-EDS) image of Cu-Pd-Ga NP with an individual elemental map of Ga, Pt, O, and Cu, (b) XPS spectrum of the Ga $2p$  region, Cu $2p$  region and Pd $3d$  region in Cu-Pd-Ga (3.0:0.5:96.5) alloy NPs, (c,d) XPS survey scan of Cu-Pt-Ga and Cu-Pd-Ga.

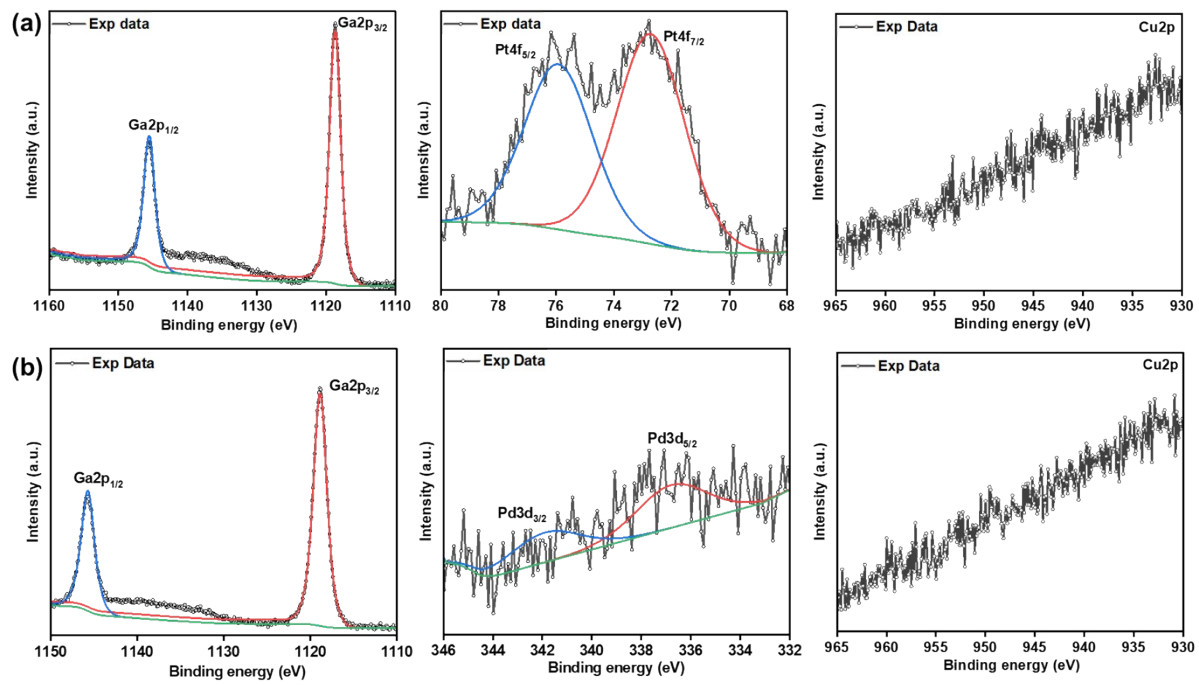


**Figure S4.** Surface and elemental analysis of CC-Cu-Pt-Ga and CC-Cu-Pd-Ga, (a) Ga2p region and Pt 4f region over CC-Cu-Pt-Ga catalyst, (b) CC-Cu-Pd-Ga XPS spectrum of Ga2p region and Pd3d region.

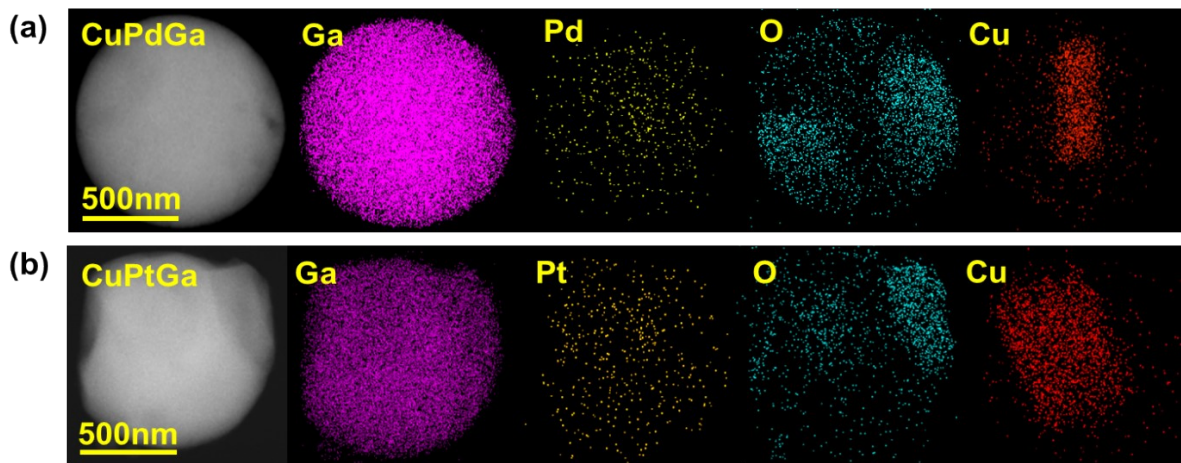


**Figure S5.** Dark field transmission electron microscopy (DF-TEM) images of fresh and spent ternary alloy NPs after methane decomposition, (a) CC-Cu-Pd-Ga with elemental mapping images of Ga, Pd, O and Cu, (b) CC-Cu-Pt-Ga catalyst TEM images along an elemental map of Ga, O, Pt and Cu.

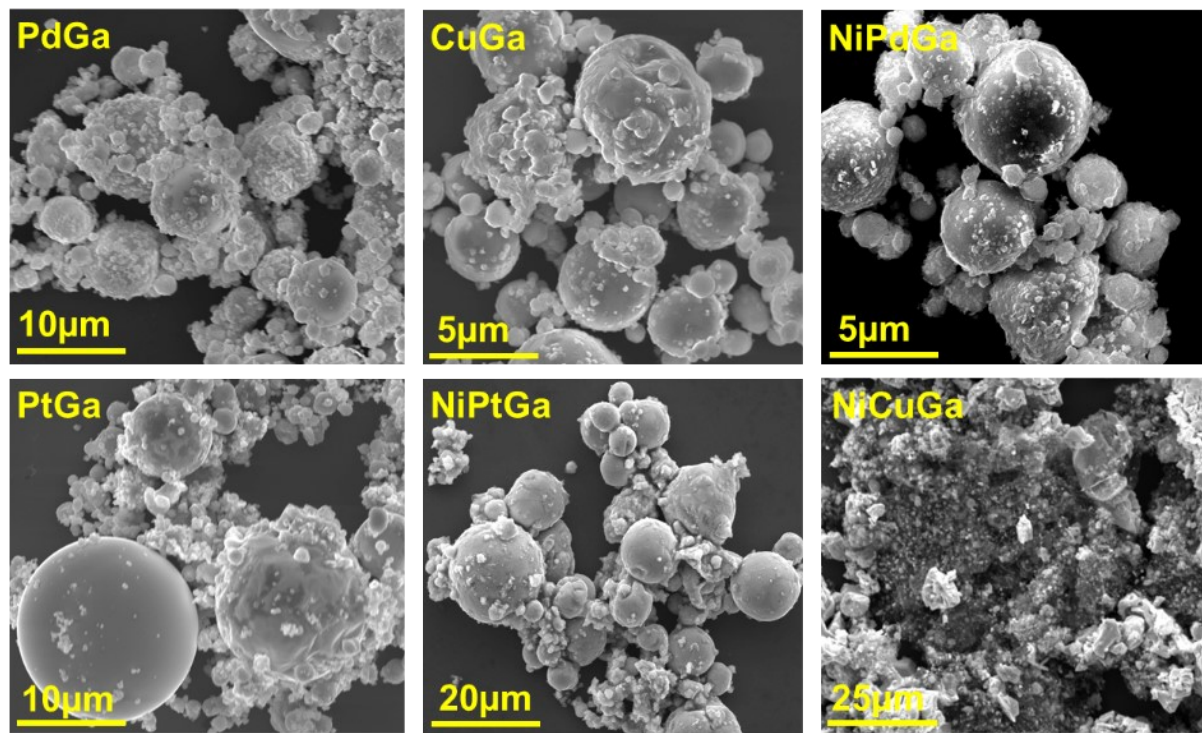


**Figure S6.** SEM imaging of binary and ternary NPs (Pd-Ga, Cu-Ga, Pt-Ga, Ni-Pt-Ga, Ni-Pd-Ga, and Ni-Cu-Ga) after methane pyrolysis and carbon formation.

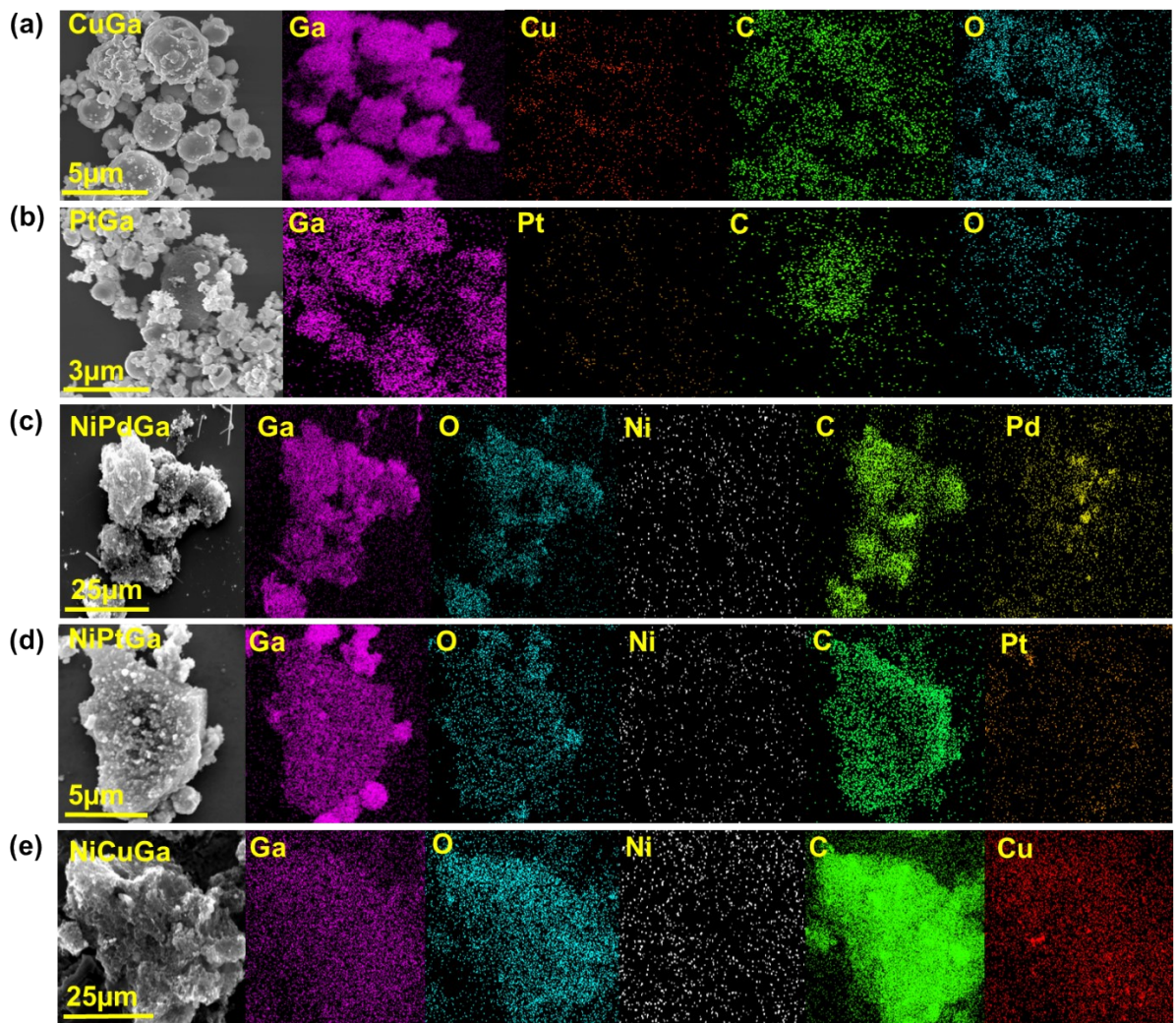


**Figure S7.** SEM-EDS of binary and ternary alloy NPs after methane decomposition at 600°C,  
(a) Cu-Ga (03:97), (b) Pt-Ga (0.5:99.5), (c) Ni-Pd-Ga (3.0:0.5:96.5), (d) Ni-Pt-Ga  
(3.0:0.5:96.5), (e) Ni-Cu-Ga (3.0:03:94).

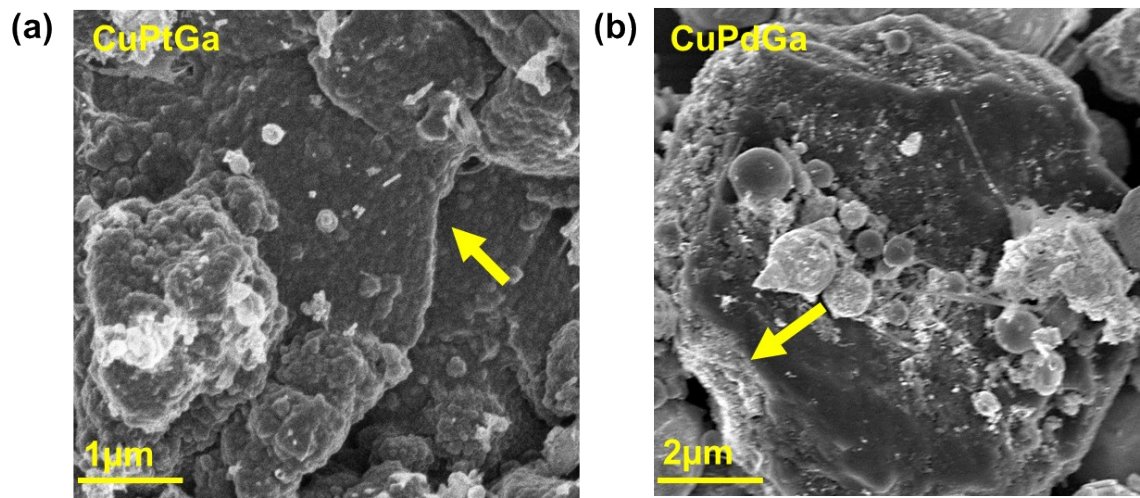


**Figure S8.** SEM imaging of rod-like structures formed during methane pyrolysis over the following catalysts: (a) Cu-Pt-Ga, (b) Cu-Pd-Ga.

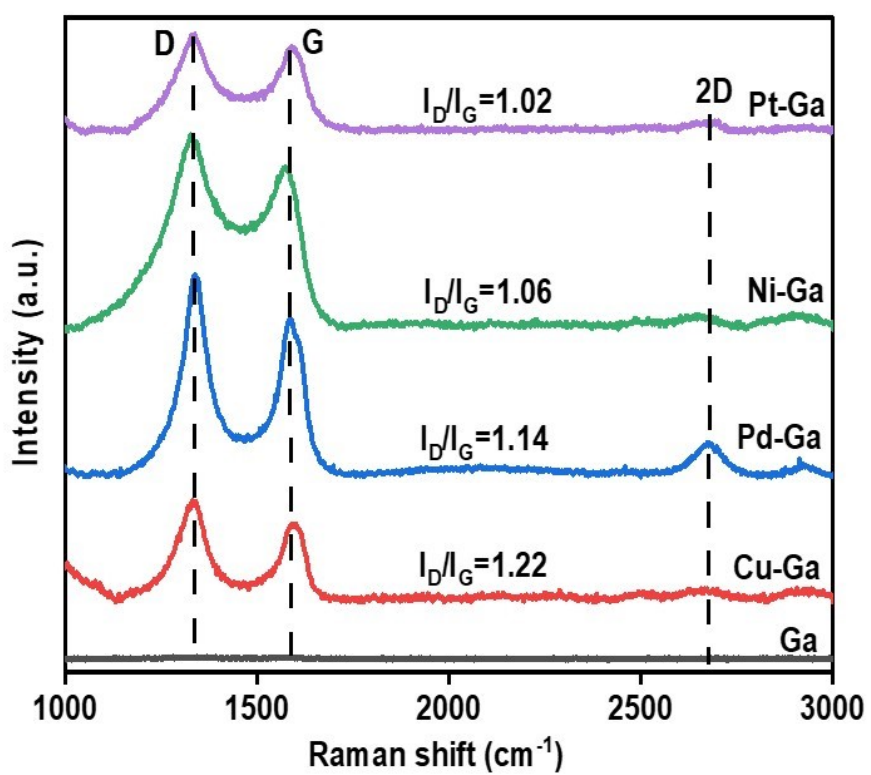


**Figure S9.** RAMAN spectra of binary alloy NPs after methane decomposition at 600 °C for 180 min.

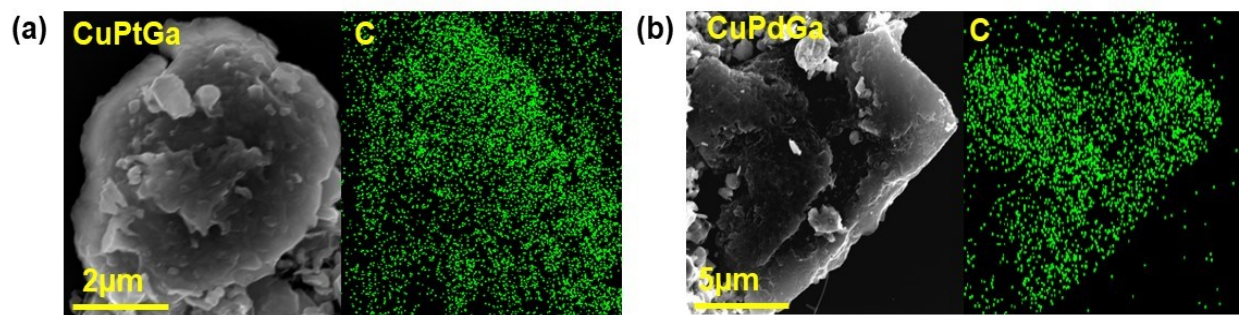


**Figure S10.** (a) SEM-EDS of graphitic carbon product formed after methane pyrolysis over Cu-Pd-Ga (3.0:0.5:96.5) NPs, (b) Product graphitic carbon by Cu-Pt-Ga (3.0:0.5:96.5) NPs.

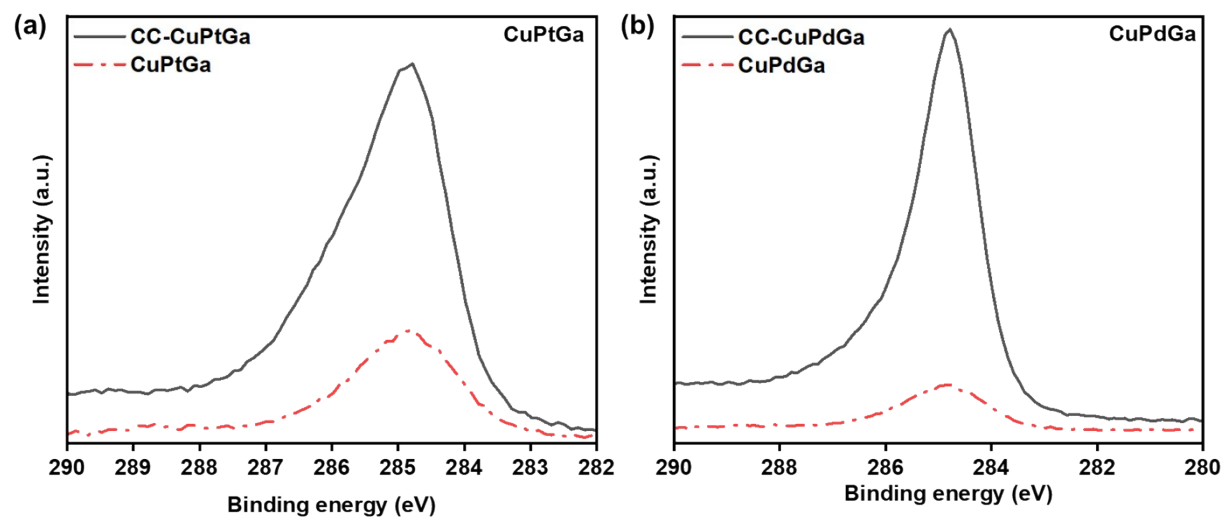


**Figure S11.** XPS spectrum of carbon region (C1s) detected before and after carbon coating by the following catalysts: (a) Cu-Pt-Ga and (b) Cu-Pd-Ga.

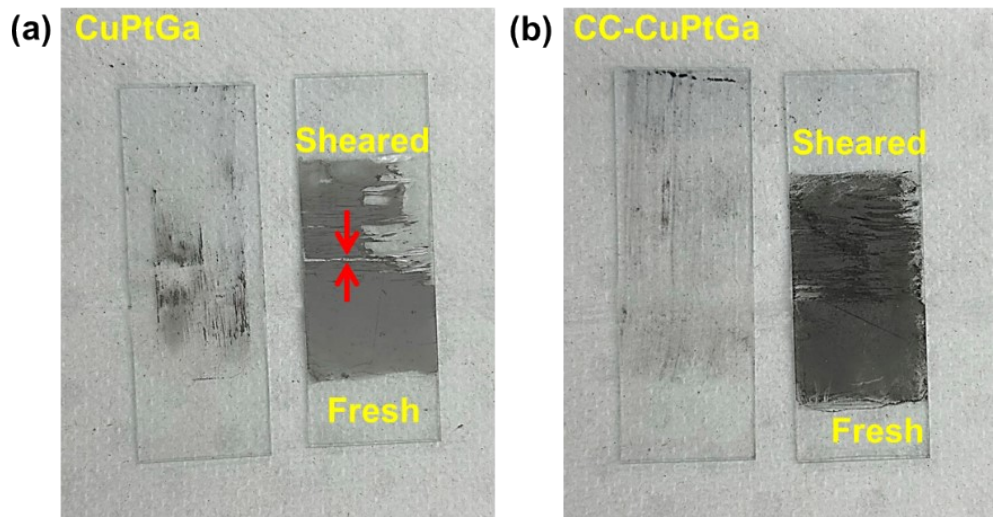


**Figure S12.** (a, b) Comparison of Cu-Pt-Ga and CC-Cu-Pt-Ga before and after mechanical stress testing (MS).

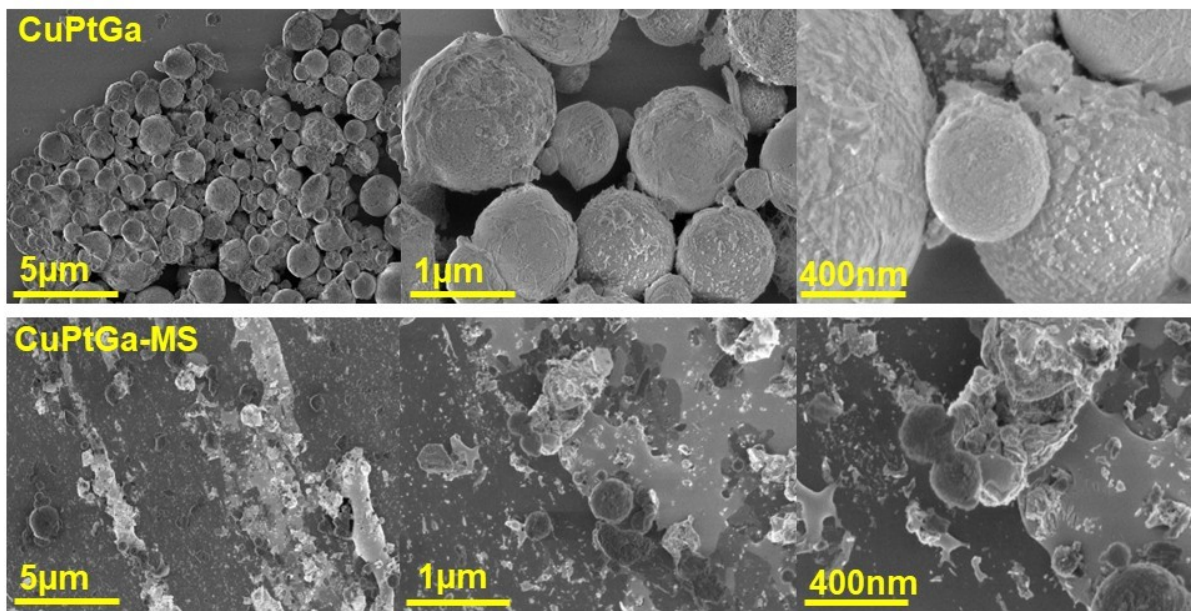


**Figure S13.** SEM imaging of Cu-Pt-Ga nanoparticles before and after mechanical stress testing (MS).

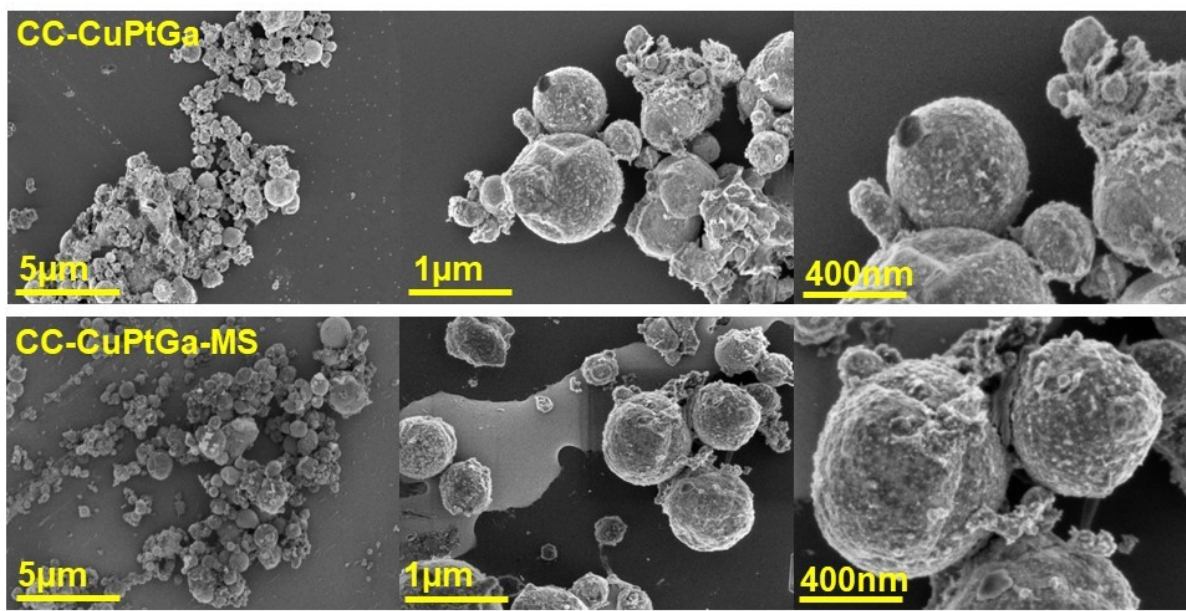


**Figure S14.** SEM imaging of CC-Cu-Pt-Ga nanoparticles before and after mechanical stress testing (MS).

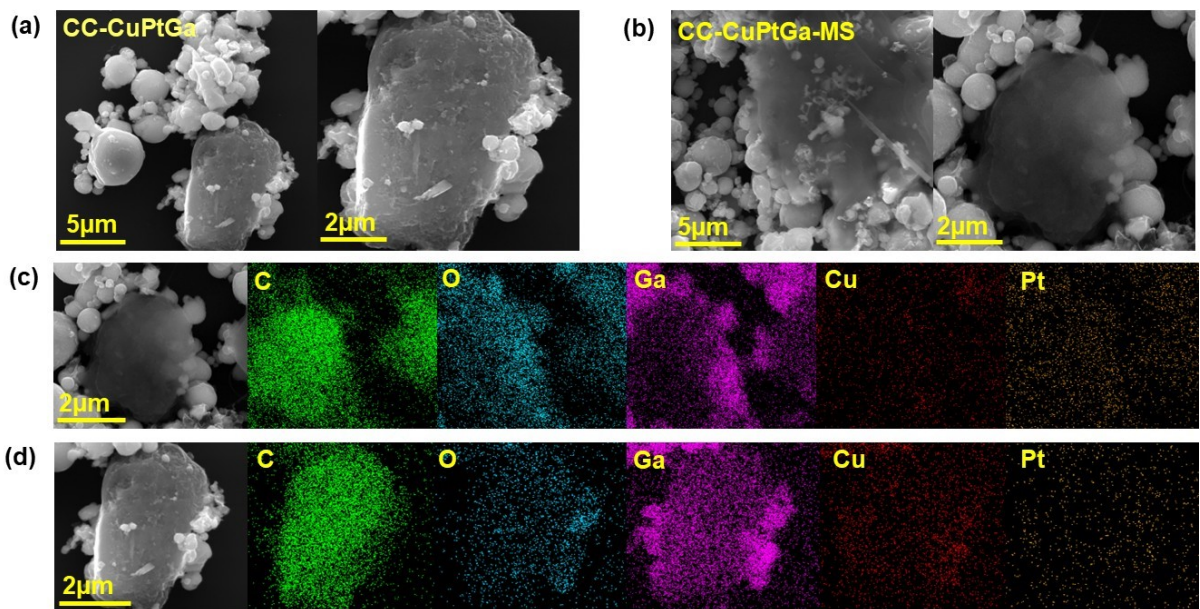


**Figure S15.** SEM imaging of carbon flake in (a) CC-Cu-Pt-Ga and (b) CC-Cu-Pt-Ga after mechanical stress testing (MS), (c, d) SEM-EDS elemental mapping of carbon product present in (c) CC-Cu-Pt-Ga and (d) CC-Cu-Pt-Ga after mechanical stress testing (MS).

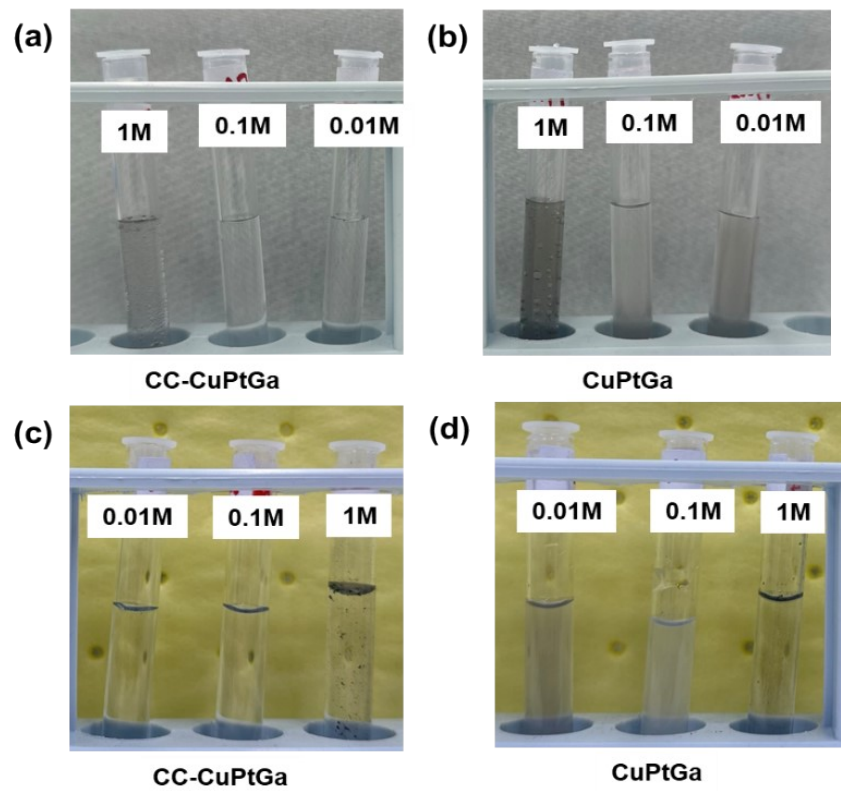


**Figure S16.** Cu-Pt-Ga and carbon-coated Cu-Pt-Ga (CC-Cu-Pt-Ga) nanoparticles after different hours of HCl exposure (a, b) 3hrs and (c, d) 48hrs.

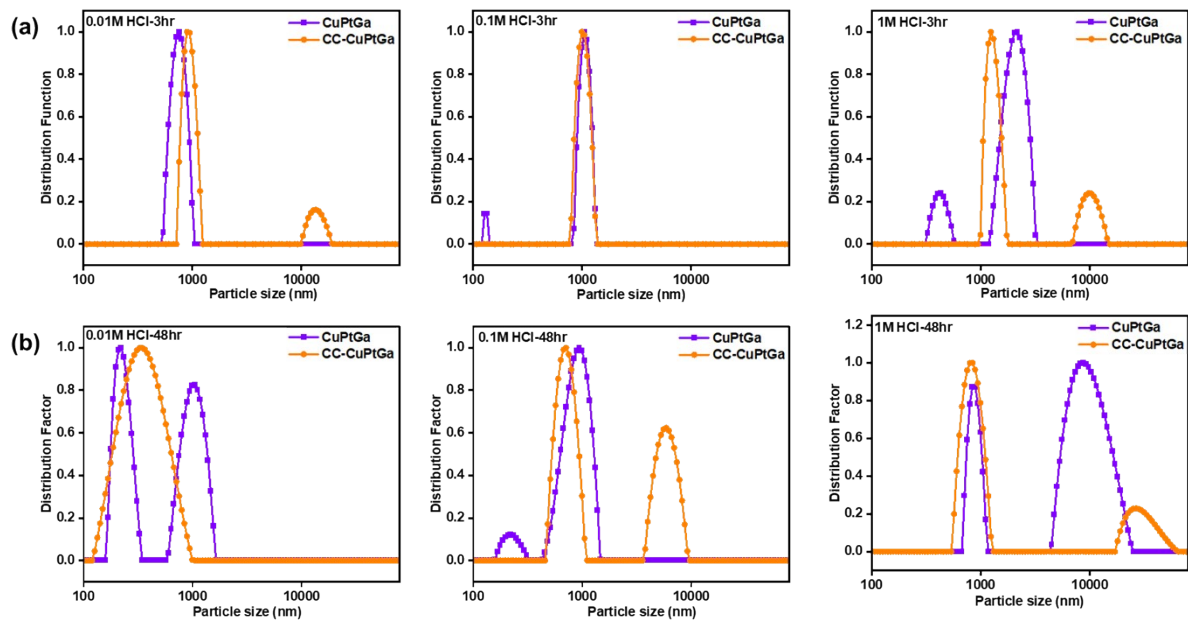


**Figure S17.** Dynamic light scattering (DLS) droplet size distribution of Cu-Pt-Ga and CC-Cu-Pt-Ga after following durations to acidic media (0.1M, 0.01M and 1M HCl solution): (a) 3 hrs exposure and (b) 48 hrs exposure.

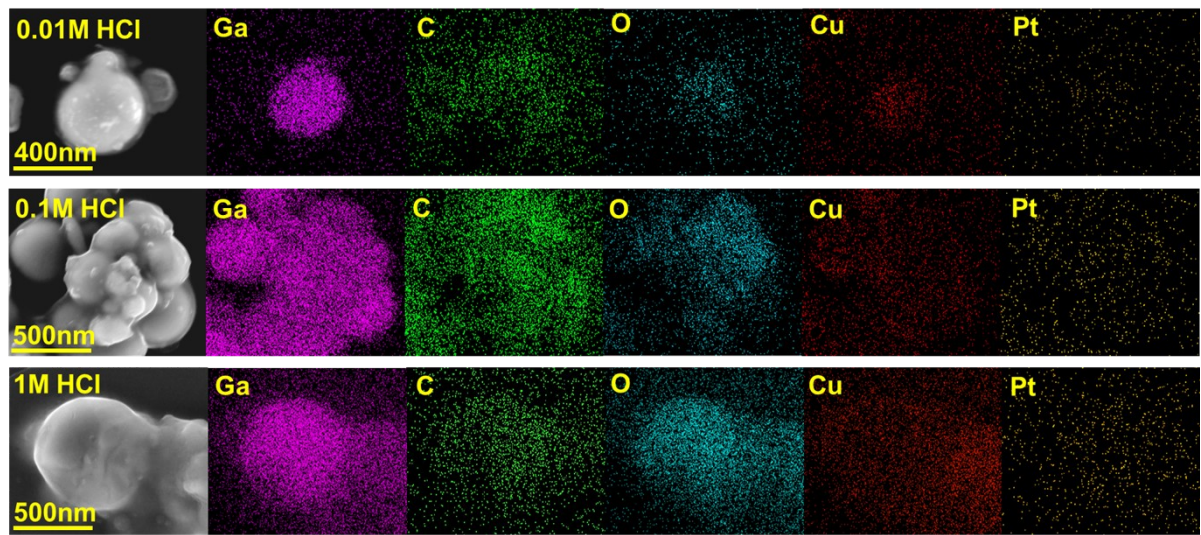


**Figure S18.** SEM-EDS of CC-Cu-Pt-Ga alloy NPs after 3 hrs. exposure to acidic media (0.01M, 0.1M and 1M HCl).